PAPER

Vinylpyrroles: solid-state structures and aggregation-induced emission properties†

Toru Okawara, [ID] *[a] Yurina Matsufuji,[b] Kouhei Mizuno,[a] Kenji Takehara,[a] Toshihiko Nagamura [ID] [ac] and Seiji Iwasa[d]

An aggregation-induced emission chromophore, vinylpyrrole, was prepared from a formylpyrrole derivative, Meldrum's acid, and 1,3-dimethylbarbituric acid. The optical properties of the chromophore both in the solution and solid states were investigated by UV-vis and fluorescence spectroscopy. Single crystal X-ray diffraction measurements revealed that the dimethylbarbituric acid adduct formed a J-aggregate in the solid and resulted in higher fluorescence quantum yield compared to the Meldrum's acid adduct. Emission enhancement was found to occur by the restriction of molecular rotation in the solid state.

Introduction

Organic luminescence compounds have attracted significant attention due to their importance in applications such as organic light-emitting diodes and fluorescence probes.[1,2] In general, the aggregation or strong intermolecular interactions between luminophores causes a loss of the luminescence quantum yield due to energy migration and/or excimer formation, which is otherwise known as aggregation caused quenching (ACQ) or concentration quenching. As such, the majority of luminescence studies are performed in dilute solutions or solid matrices; this is usually accompanied by drawbacks such as difficulties in sealing the solution, or a low luminescence intensity for practical applications. In 2001, an aggregation-induced emission (AIE) dye that exhibits intense luminescence in the solid or aggregated states was reported.[3–6] Since the first "AIEgen" was developed, a number of organic compounds, namely tri- and tetraarylethenes,[7–13] cyanostilbene,[14–16] and carborane,[17–19] were found to exhibit AIE properties, and have been utilised in practical light emitting devices

and sensors.[10,20–23] In the isolated state, AIEgens lose their excitation energy due to intramolecular rotation of their phenyl rings. In contrast, in the aggregated state, the free rotation of these phenyl rings is restricted by intermolecular interactions, and so the phenyl rings can prevent strong interactions between the luminophores. This results in intense emissions in the solid and/or aggregated states. To date, numerous AIE molecules with diverse core structures have been developed, where the majority of quenching mechanisms in solution is dependent on the phenyl group, and investigations into the rotatory motion of aromatic heterocyclic groups are still very limited. For example, pyrrole, an aromatic heterocyclic compound, is found in various natural compounds, and plays important biological roles.[24–27] In addition, recent publications reported pyrrole-containing AIE molecules,[13,28–31] while in our group, we recently achieved blue to red luminescent bipyrroles through the incorporation of electron-deficient vinyl groups.[32–34] The cyclic terminal moieties such as Meldrum's acid and 1,3-dimethylbarbituric acid at the vinyl terminal are advantageous for high fluorescence quantum yield. Thus, herein we report the preparation of vinylpyrroles **1** and **2** (Scheme 1) that exhibit AIE properties in

[a]Department of Creative Engineering, National Institute of Technology, Kitakyushu College, Shii 5-20-1, Kokuraminami-ku, Kitakyushu, Fukuoka, 802-0985, Japan. E-mail: okawara@kct.ac.jp

[b]Advanced School of Creative Engineering, National Institute of Technology, Kitakyushu College, Shii 5-20-1, Kokuraminami-ku, Kitakyushu, Fukuoka, 802-0985, Japan

[c]Advanced Manufacturing Research Institute Biochemical Process Research Group, National Institute of Advanced Industrial Science and Technology (AIST), 807-1 Shuku-machi, Tosu, Saga 841-0052, Japan

[d]Department of Applied Chemistry and Life Science, Toyohashi University of Technology, 1-1 Tempaku-cho, Toyohashi, Aichi 441-8580, Japan

† Electronic supplementary information (ESI) available: Spectroscopy, crystallographic data, absolute quantum yield, and initial coordinates for the TD-DFT calculations. CCDC 1911989 and 1911990. For ESI and crystallographic data in CIF or other electronic format see DOI: 10.1039/c9ra04088a
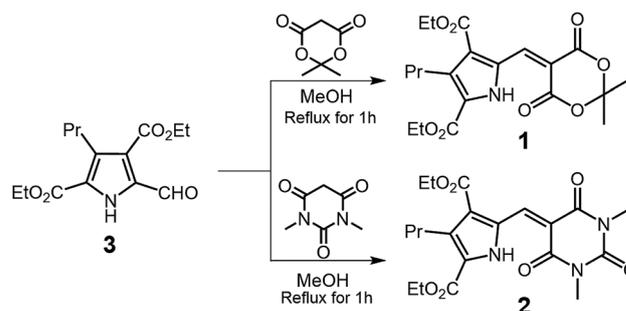
Scheme 1 Synthetic route to compounds **1** and **2**.

a tetrahydrofuran (THF)/water solvent system. The solid state photophysical properties and crystal structures are also discussed.

Experimental section

Materials and instruments

All reagents and solvents were purchased from FUJIFILM Wako Pure Chemical Corporation or Tokyo Chemical Industry Co., Ltd. and used as received unless otherwise stated. Compounds **3** was synthesized according to the literature.[35] UV-vis absorption spectra in solution were recorded on a JASCO V-570 spectrophotometer. Diffuse-reflectance spectra were measured by a JASCO V-550 spectrophotometer. Emission spectra were measured by a JASCO FP8500 or Hitachi F7000 spectrophotometer. ^1H and ^{13}C NMR spectra were obtained at 25 °C on a JEOL ECS-400 FT-NMR spectrometer with tetramethylsilane as an internal standard of the chemical shift. Infrared (IR) spectra were recorded on a JASCO FT/IR-410 spectrometer. Electrospray ionization time of flight mass (ESI-TOF-MS) spectrometry were carried out with JEOL JMS-T100CS spectrometer using methanol/dichloromethane as a solvent system. CHN elemental analysis was performed at Center for Instrumental Analysis of Kyushu Institute of Technology. Absolute photoluminescence quantum yields were determined by using a Hamamatsu Absolute PL Quantum Yield Spectrometer C11347 Quantaurus-QY (400–1100 nm) which equipped with an integrating sphere.

Synthesis

General procedure. In a round bottomed flask, 70 mg (0.25 mmol) of diethyl 5-formyl-3-propyl-2,4-pyrroledicarboxylate (**3**) and 2.5 mmol of Meldrum's acid or 1,3-dimethylbarbituric acid were dissolved in 10 mL of methanol. The solution was refluxed for 30 min. The reaction mixture was cooled to room temperature and 20 mL of water was added to the mixture. Resulting yellow precipitates were collected by filtration and washed with water. The product was purified by a neutral alumina.

Diethyl 5-[(2,2-dimethyl-4,6-dioxo-1,3-dioxan-5-ylidene) methyl]-3-propyl-1H-pyrrole-2,4-dicarboxylate (1). Yield: 89 mg (88%). Elemental analysis found: C 59.07, H 6.14, N 3.56, calcd ($C_{20}H_{25}NO_8$) C 58.96, H 6.19, N 3.44; ^1H NMR (400 MHz, 298 K, $CDCl_3$, ppm): $\delta = 13.49$ (s, 1H, NH), 9.34 (s, 1H, vinyl-CH), 4.43 (q, $J = 7.2$ Hz, 4H, $-CH_2CH_3$), 3.10 (m, 2H, $-CH_2CH_2CH_3$), 1.79 (s, 6H, $>C(CH_3)_2$), 1.58 (m, $-CH_2CH_2CH_3$), 1.45 (t, $J = 7.2$ Hz, 6H, $-CH_2CH_3$), 0.98 (t, $J = 7.4$ Hz, 3H, $-CH_2CH_2CH_3$); ^{13}C NMR (100 MHz, 298 K, $CDCl_3$, ppm) $\delta = 163.75$, 162.82, 159.61, 143.35, 137.61, 128.56, 126.56, 124.99, 108.48, 105.03, 61.46, 61.18, 27.50, 27.18, 24.32, 14.32, 14.18, 14.15; IR (KBr) wavenumber cm^{-1}: 2979 (ν_{C-H}), 2959 (ν_{C-H}), 2870 (ν_{C-H}), 1748 ($\nu_{C=O}$), 1708 ($\nu_{C=O}$); ESI-TOF-MS (CH_3OH/CH_2Cl_2): $m/z = $ 408.17 ([M + H]$^+$).

Diethyl 5-[(1,3-dimethyl-2,4,6-trioxotetrahydropyrimidin-5(2H)-ylidene)methyl]-3-propyl-1H-pyrrole-2,4-dicarboxylate (2). Yield: 94 mg (90%). Elemental analysis found: C 56.98, H 5.89, N 9.86, calcd ($C_{20}H_{25}N_3O_7$) C 57.27, H 6.01, N 10.02; ^1H NMR (400 MHz, 298 K, $CDCl_3$, ppm): $\delta = 14.16$ (s, 1H, NH), 9.41 (s, 1H, vinyl-CH), 4.44, (q, $J = 7.2$ Hz, 4H, $-CH_2CH_3$), 3.47, 3.43 (s, 6H, $>NCH_3$), 3.09 (m, 2H, $-CH_2CH_2CH_3$), 1.62 (m, 2H, $-CH_2CH_2CH_3$), 1.47, 1.45 (t, $J = 7.6$ Hz, 6H, $-CH_2CH_3$), 0.98 (t, $J = 7.4$ Hz, 3H, $-CH_2CH_2CH_3$), ^{13}C NMR (100 MHz, 298 K, $CDCl_3$, ppm) $\delta = 163.71$, 163.22, 162.30, 160.21, 151.02, 143.02, 137.60, 129.33, 126.22, 124.84, 112.60, 61.43, 61.07, 29.19, 28.85, 27.32, 24.39, 14.26, 14.17; IR (KBr) wavenumber cm^{-1}: 2961 (ν_{C-H}), 2933 (ν_{C-H}), 2871 (ν_{C-H}), 1723 ($\nu_{C=O}$), 1702 ($\nu_{C=O}$), 1671 ($\nu_{C=O}$), 1646 ($\nu_{C=O}$); ESI-TOF-MS (CH_3OH/CH_2Cl_2): $m/z = 420.20$ ([M + H]$^+$).

X-ray crystallography

X-ray diffraction data were collected using a Bruker SMART APEX CCD diffractometer (for **1**) and Rigaku XtaLAB mini diffractometer (for **2**) both equipped with graphite-monochromated Mo Kα radiation ($\lambda = 0.71073$ Å) from a fine-focus sealed tube. Each single crystals of **1** or **2** was mounted on a glass fiber and the data frames were integrated using *SAINT* or *CrysAlisPro*.[36,37] The integrated data were merged to give a unique data set for the structure determination. *SADABS* or *CrysAlisPro* were used for absorption correction.[38] The structure was solved by a direct method and refined by the full-matrix least-squares method on all F^2 data using the *Olex2* suite of program.[39] All non-hydrogen atoms were anisotropically refined. Hydrogen atoms were placed at geometrically idealized positions and constrained to ride on their parent atoms with $U_{iso}(H) = 1.2U_{eq}(NH, CH$ and $CH_2)$ and $U_{iso}(H) = 1.5U_{eq}(CH_3)$. Crystallographic data have been deposited with the Cambridge Crystallographic Data Centre as supplementary publication no. CCDC 1911989 and 1911990.†

Computational study

Molecular structures and electronic transitions were evaluated by time-dependent density functional theory (TD-DFT) calculations. The initial coordinates of compounds **1** and **2** used for the TD-DFT calculations were obtained directly from the X-ray crystal structures. The TD-DFT calculations were performed using the *Gaussian 09* suite.[40] The camB3LYP/6-31G(d, p) was used as the basis set. The solvent effect was considered in THF by the polarisable continuum model using the integral equation formalism variant (IEFPCM).

Aggregation-induced emission behaviour in THF/water mixture

Stock solutions of **1** and **2** in THF with a concentration of 1.0×10^{-3} M were prepared. The aggregates were freshly prepared by adding water into the pyrrole solutions to make a total amount of 5 mL mixture. For example, the water fraction of 80% mixture including 1.0×10^{-4} M of a dye was prepared by 0.50 mL of the stock solution and diluted with 0.50 mL of THF followed by addition of 4.0 mL water. The fluorescence spectra were recorded by Hitachi F7000 spectrophotometer. Fluorescence and excitation slit widths were set to 5.0 nm and 10.0 nm, respectively. All spectra were recorded under 365 nm excitation wavelength.

Viscosity effects on the UV-vis and fluorescence spectra of 2

50 μL of a stock solution of **2** in CH₂Cl₂ with a concentration of 1.0×10^{-3} M was stored in glass tubes. After removal of the solvent, the residue was re-dissolved in 5 mL of methanol/glycerol solvents (100/0, 50/50, 40/60, 30/70, 20/80, 10/90 and 5/95, v/v). UV-vis spectra indicates there are no precipitates in all of the solutions (Fig. S1 and S2†).

Results and discussion

The target compounds were obtained from diethyl 5-formyl-3-propyl-2,4-pyrroledicarboxylate (**3**), Meldrum's acid, and 1,3-dimethylbarbituric acid in refluxing methanol (Scheme 1).[41] The crude products were precipitated from the reaction mixtures by the addition of water. These precipitates were collected and washed with water to yield analytically pure products **1** and **2** in excellent yields (88 and 90%, respectively). Both compounds were characterised by standard spectroscopic methods and CHN elemental analysis. The ¹H NMR spectra of the products recorded in CDCl₃ suggested that intramolecular hydrogen bonding between the NH and carbonyl groups stabilised the planar structure of the molecules in solution. We note that the NH singlet peaks of **1** and **2** were observed between 13 and 15 ppm, which is significantly downfield shifted compared with the corresponding peaks for the starting aldehyde. Similar trends can be found in previously reported analogues.[33,34]

To obtain further structural insights, X-ray diffraction analysis was performed on compounds **1** and **2**.‡ For this purpose, single crystals of **1** and **2** were obtained from dichloromethane/n-heptane and dichloromethane/n-hexane solutions with monoclinic C2/c and P2₁/c symmetries for **1** and **2**, respectively. The obtained ORTEP diagrams together with the atom labelling and molecular packing diagrams are displayed in Fig. 1 and 2. Crystallographic details and selected molecular geometries are provided in the ESI.† It was found that in the solid state, compounds **1** and **2** adopted planar structures, as expected from the spectroscopic results. The torsion angles between C1–C5–C6–C7 were only 3.47° and 1.77° for **1** and **2**, respectively. Indeed, it was clear that intramolecular hydrogen bonding between N1–H1⋯O1 ($d_{N1⋯O1}$ = 2.696 Å for **1**, and 2.613 Å for **2**) gives rise to the planar conformation in the solid-state. The hydrogen bonding interactions are often found in the bipyrrole systems.[33,34,42] Although the molecular structures were similar, the intermolecular interactions present in **1** and **2** were different. The shortest inter-layer distance in **1**, which is defined as the distance between the mean plane of the pyrrole ring (i.e., N1, C1, C2, C3, and C4), was determined to be 3.50 Å. In addition, as shown in Fig. 2a, two molecules of **1** formed an
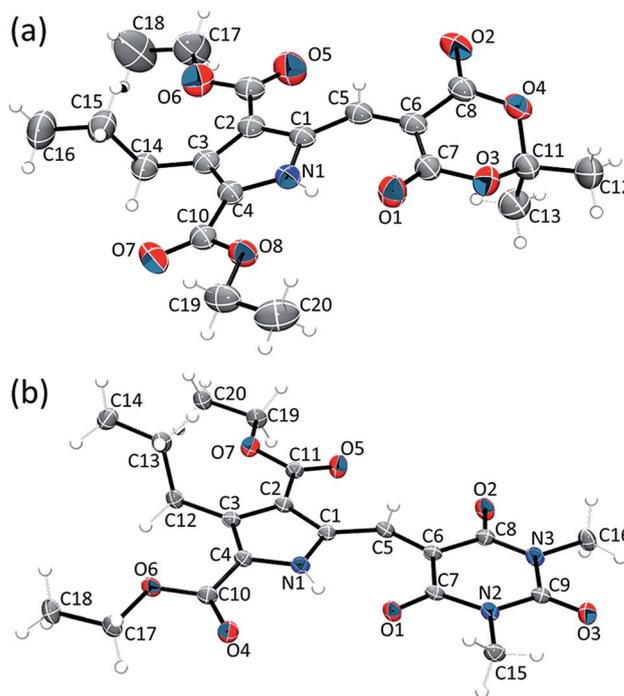

Fig. 1 Crystal structures of 1 and 2. The thermal ellipsoids were drawn at 30 and 50% for (a) 1 and (b) 2, respectively.

antiparallel dimer-like aggregate. In contrast, compound **2** formed an infinite π–π stack along the b-axis, with an interplanar distance of 3.46 Å (Fig. 2b). The slip angle of the π–π interactions was calculated to be 41.5°, which corresponds to the J-aggregate.[43]

The optical properties of **1** and **2** recorded in both the solution-state (i.e., in THF) and the solid-state are shown in Fig. 3, and the relevant photophysical data are summarised in Table 1. As shown, the absorption bands of **1** and **2** in THF are located at ∼400 nm. TD-DFT calculations revealed that the absorption bands in THF were estimated to appear at 417.76 and 422.14 nm, for **1** and **2**, respectively (Table 1). Both bands were derived from the HOMO–LUMO transitions. Intramolecular charge transfer could be ruled out since no obvious correlations were observed in the Mataga–Lippert plot (Fig. S3–S5†).[17] Compounds **1** and **2** were virtually nonfluorescent in solution, i.e., the absolute quantum yields were <1%. In
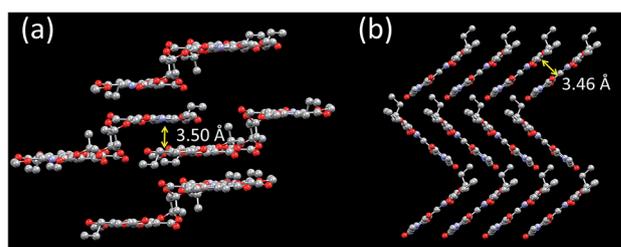
Fig. 2 Crystal structures of 1 and 2. The thermal ellipsoids were drawn at 30 and 50% for (a) 1 and (b) 2, respectively.

addition, compound **2** exhibited a relatively longer absorption and fluorescence due to the π-extension effect caused by the fully sp²-hybridised barbituric moiety.[33,34] It is worth noting that the Stokes shift values of **1** and **2** were >3000 cm⁻¹, which is notably larger than those of π-conjugated compounds. This was attributed to an excited-state feature of pyrrole derivatives, *i.e.*, the single bond between the pyrrole ring and the adjacent π-system.[44,45] In contrast to the solution properties, the solid-state fluorescence maxima of compounds **1** and **2** are located at a more red-shifted wavelengths in comparison to the emission obtained in the THF solutions ($\lambda_{FL,solid}$ = 544 and 493 nm for **1** and **2**, respectively). The large photoluminescence quantum yield of **2** can be explained by the formation of the J-aggregate, as described above. Indeed, it has been reported that this type of aggregation is advantageous for solid-state fluorophores.[14,16] In addition, compound **1** exhibited a relatively large Stokes shift owing to weak intermolecular interactions in the solid-state.

As shown in Fig. 4 and 5, the vinylpyrroles exhibited a drastic increase in fluorescence intensity from the molecularly dissolved state in THF to the aggregated state in the THF-water mixtures. Indeed, compounds **1** and **2** exhibited negligible fluorescence in the THF solution, whereas the fluorescence

Table 1 Photophysical parameters for **1** and **2** under aerobic conditions

		1	**2**
THF	λ_{Abs}	401 nm	412 nm
	λ_{FL}	459 nm	473 nm
	Stokes shift	3152 cm⁻¹	3130 cm⁻¹
	Φ_{FL}	<0.01	<0.01
	Calcd λ_{Abs}[a]	417.76 nm	422.14 nm
	Transition[a]	108 (HOMO) −109 (LUMO)	111 (HOMO) −112 (LUMO)
	Oscillator strength[a]	0.7541	0.9041
Solid	λ_{Abs}	424 nm	434 nm
	λ_{FL}	544 nm	493 nm
	Stokes shift	5203 cm⁻¹	4757 cm⁻¹
	Φ_{FL}	0.10	0.24

[a] TD-DFT calculations were performed using the *Gaussian 09* suite and the camB3LYP/6-31G(d, p) basis set. The solvent effect was considered in THF by the polarisable continuum model using the integral equation formalism variant (IEFPCM).

intensity increased significantly with water fractions >80 vol%. Since **1** and **2** are insoluble in water, the increased water fraction leads to their precipitation. Furthermore, we note that the fluorescence spectra of the two compounds in the presence of 90 vol% water were similar to their solid-state PL spectra, although one shoulder peak had disappeared. Moreover, compound **1** showed a relatively large bathochromic shift upon aggregation compared with compound **2**. These observations indicate the occurrence of AIE in these vinylpyrroles.

We subsequently examined the effect of viscosity on the fluorescence of **2**, and thus, the fluorescence intensity as a function of the glycerol (934 mPa s, 25 °C) content in methanol (0.544 mPa s, 25 °C) was plotted as shown in Fig. 6.[46] As
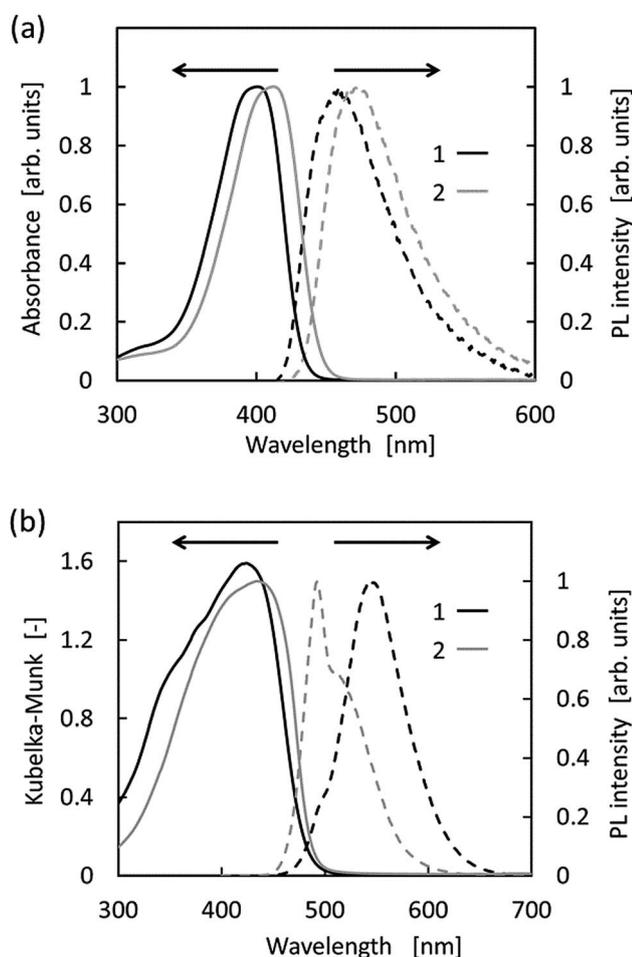

Fig. 3 Absorption (solid lines) and photoluminescence (PL) (broken lines) spectra of **1** (black) and **2** (grey) in (a) THF (*i.e.*, the solution-state) and (b) the solid-state.
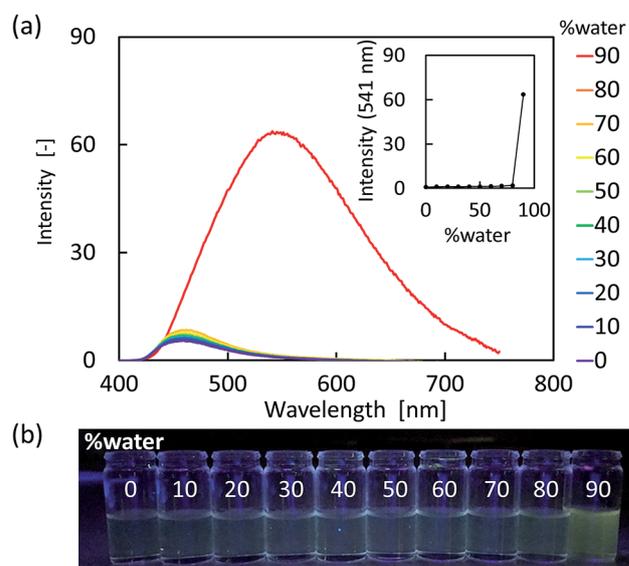

Fig. 4 (a) PL spectral changes of **1** (1 × 10⁻⁴ M) based on the water fraction present in the THF solution. (b) Photographic images of **1** in the THF–water mixtures.

Fig. 5 (a) PL spectral changes of **2** (1×10^{-4} M) based on the water fraction present in the THF solution. (b) Photographic images of **2** in the THF–water mixtures.
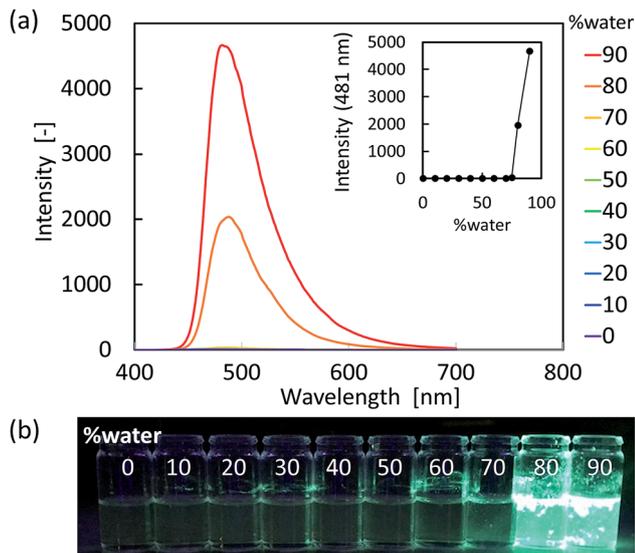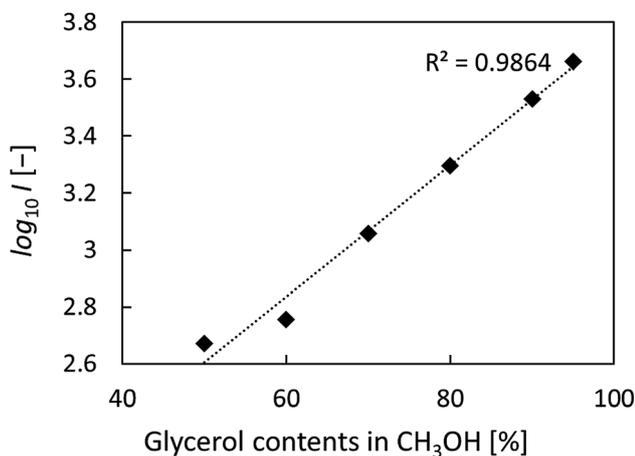

Fig. 6 Photoluminescence peak intensity of **2** *vs.* the composition of the glycerol–methanol mixtures (1×10^{-5} M).

indicated, $\log_{10} I$ of the fluorescence spectrum increased linearly upon increasing the glycerol content from 50 to 95 vol%. Such fluorescence enhancement at higher glycerol concentrations likely results from the viscosity effect, as no baseline increase was observed for the absorption spectra, *i.e.*, no aggregates and/or precipitates were formed (Fig. S1†). This result indicates that the AIE properties of the vinylpyrroles were predominantly caused by the restriction of intramolecular rotation (RIR) mechanism. We also note that the molecular structures calculated by the TD-DFT (Fig. S16†) were likely planar due to the presence of intramolecular NH···O hydrogen bonds. Meanwhile, this hydrogen bond dissociates in the excited state and allows free rotation along the single bond between the pyrrole moiety and the electron-deficient vinyl group.

Conclusions

We herein reported the successful syntheses of pyrrole derivatives that exhibited aggregation-induced emission (AIE) behaviour in THF-water mixtures. The prepared compounds (numbered **1** and **2**) were virtually nonfluorescent in organic solvents, but were highly luminous in the solid-state. Compound **1** produced dimer-like aggregates in the crystal form while compound **2** gave J-type infinite aggregates. In addition, it was found that the intermolecular interactions dominating in each compound directly influenced their photophysical properties. More specifically, compound **2** exhibited relatively short yet intense photoluminescence due to strong intermolecular interactions and J-aggregation formation in the solid-state. These strong interactions are also likely to be advantageous in terms of decreasing the non-radiative relaxations of the excited state. Furthermore, studies into the effect of viscosity revealed that the aggregation-induced emission behaviour of the compounds can be explained by the restriction of intramolecular rotation mechanism. These results confirm that we successfully proposed a novel molecular design for AIE molecules based on the rotation of aromatic heterocyclic compounds that do not contain phenyl rings. We believe that this result will promote further exploration of AIE-active chromophores. Additional studies of AIE-active aromatic heterocyclic compounds are currently ongoing in our groups.

Conflicts of interest

There are no conflicts to declare.

Acknowledgements

Notes and references

1 *Organic Light-Emitting Devices: Synthesis Properties and Applications*, ed. K. Müllen and U. Scherf, Wiley-VCH, Weinheim, 2006.
2 A. C. Grimsdale, K. Leok Chan, R. E. Martin, P. G. Jokisz and A. B. Holmes, *Chem. Rev.*, 2009, **109**, 897–1091.
3 J. Luo, Z. Xie, J. W. Y. Lam, L. Cheng, H. Chen, C. Qiu, H. S. Kwok, X. Zhan, Y. Liu, D. Zhu and B. Z. Tang, *Chem. Commun.*, 2001, 1740–1741.
4 Z. Zhao, B. He and B. Z. Tang, *Chem. Sci.*, 2015, **6**, 5347–5365.
5 J. L. Mullin, H. J. Tracy, J. R. Ford, S. R. Keenan and F. Fridman, *J. Inorg. Organomet. Polym. Mater.*, 2007, **17**, 201–213.

6 X.-L. Peng, S. Ruiz-Barragan, Z.-S. Li, Q.-S. Li and L. Blancafort, *J. Mater. Chem. C*, 2016, **4**, 2802–2810.

7 T. Sajima, T. Nagamura, T. Okawara and K. Takehara, *Sci. Adv. Mater.*, 2015, **7**, 981–984.

8 R. Hu, C. F. A. Gómez-Durán, J. W. Y. Lam, J. L. Belmonte-Vázquez, C. Deng, S. Chen, R. Ye, E. Peña-Cabrera, Y. Zhong, K. S. Wong and B. Z. Tang, *Chem. Commun.*, 2012, **48**, 10099–10101.

9 H. Shi, R. T. Kwok, J. Liu, B. Xing, B. Z. Tang and B. Liu, *J. Am. Chem. Soc.*, 2012, **134**, 17972–17981.

10 M. Wang, G. Zhang, D. Zhang, D. Zhu and B. Z. Tang, *J. Mater. Chem.*, 2010, **20**, 1858–1867.

11 J. Wang, J. Mei, R. Hu, J. Z. Sun, A. Qin and B. Z. Tang, *J. Am. Chem. Soc.*, 2012, **134**, 9956–9966.

12 Z. Zhao, J. W. Y. Lam and B. Z. Tang, *J. Mater. Chem.*, 2012, **22**, 23726–23740.

13 K. Garg, E. Ganapathi, P. Rajakannu and M. Ravikanth, *Phys. Chem. Chem. Phys.*, 2015, **17**, 19465–19473.

14 B.-K. An, J. Gierschner and S. Y. Park, *Acc. Chem. Res.*, 2012, **45**, 544–554.

15 B.-K. An, S.-K. Kwon, S.-D. Jung and S. Y. Park, *J. Am. Chem. Soc.*, 2002, **124**, 14410–14415.

16 B.-K. An, D.-S. Lee, J.-S. Lee, Y.-S. Park, H.-S. Song and S. Y. Park, *J. Am. Chem. Soc.*, 2004, **126**, 10232–10233.

17 K. Kokado and Y. Chujo, *J. Org. Chem.*, 2011, **76**, 316–319.

18 S.-Y. Kim, Y.-J. Cho, G. F. Jin, W.-S. Han, H.-J. Son, D. W. Cho and S. O. Kang, *Phys. Chem. Chem. Phys.*, 2015, **17**, 15679–15682.

19 R. Furue, T. Nishimoto, I. S. Park, J. Lee and T. Yasuda, *Angew. Chem., Int. Ed. Engl.*, 2016, **55**, 7171–7175.

20 Y. Hong, J. W. Y. Lam and B. Z. Tang, *Chem. Commun.*, 2009, 4332–4353.

21 J. Mei, Y. Hong, J. W. Y. Lam, A. Qin, Y. Tang and B. Z. Tang, *Adv. Mater.*, 2014, **26**, 5429–5479.

22 M. Gao, S. Li, Y. Lin, Y. Geng, X. Ling, L. Wang, A. Qin and B. Z. Tang, *ACS Sens.*, 2015, **1**, 179–184.

23 L. Zong, H. Zhang, Y. Li, Y. Gong, D. Li, J. Wang, Z. Wang, Y. Xie, M. Han, Q. Peng, X. Li, J. Dong, J. Qian, Q. Li and Z. Li, *ACS Nano*, 2018, **12**, 9532–9540.

24 P. A. Gale, *Acc. Chem. Res.*, 2006, **39**, 465–475.

25 A. P. Davis, D. N. Sheppard and B. D. Smith, *Chem. Soc. Rev.*, 2007, **36**, 348–357.

26 W. Zhou, Z. X. Jin and Y. J. Wan, *Appl. Microbiol. Biotechnol.*, 2010, **88**, 1269–1275.

27 R. Pérez-Tomás, B. Montaner, E. Llagostera and V. Soto-Cerrato, *Biochem. Pharmacol.*, 2003, **66**, 1447–1452.

28 G. Liu, D. Chen, L. Kong, J. Shi, B. Tong, J. Zhi, X. Feng and Y. Dong, *Chem. Commun.*, 2015, **51**, 8555–8558.

29 Y. Gao, G. Feng, T. Jiang, C. Goh, L. Ng, B. Liu, B. Li, L. Yang, J. Hua and H. Tian, *Adv. Funct. Mater.*, 2015, **25**, 2857–2866.

30 S. Xu, T. Liu, Y. Mu, Y.-F. Wang, Z. Chi, C.-C. Lo, S. Liu, Y. Zhang, A. Lien and J. Xu, *Angew. Chem., Int. Ed.*, 2015, **54**, 874–878.

31 X. Feng, B. Tong, J. Shen, J. Shi, T. Han, L. Chen, J. Zhi, P. Lu, Y. Ma and Y. Dong, *J. Phys. Chem. B*, 2010, **114**, 16731–16736.

32 T. Okawara, A. Doi, T. Ono, M. Abe, K. Takehara, Y. Hisaeda and S. Matsushima, *Tetrahedron Lett.*, 2015, **56**, 1407–1410.

33 R. Kawano, T. Kato, R. Fukuda, T. Okawara, K. Takehara and T. Nagamura, *ChemistrySelect*, 2016, **1**, 4144–4151.

34 T. Okawara, R. Kawano, H. Morita, A. Finkelstein, R. Toyofuku, K. Matsumoto, K. Takehara, T. Nagamura, S. Iwasa and S. Kumar, *Molecules*, 2017, **22**, 1816.

35 M. R. Johnson, D. C. Miller, K. Bush, J. J. Becker and J. A. Ibers, *J. Org. Chem.*, 1992, **56**, 4414–4417.

36 *SAINT v8.34A*, Bruker AXS Inc., Madison, Wisconsin (US), 2013.

37 *CrysAlisPro 1.171.39.34a*, Rigaku Oxford Diffraction, Oxford Diffraction Ltd., Abingdon, Oxfordshire, England, 2017.

38 G. M. Sheldrick, *SADABS, Program for Empirical Absorption Correction of Area Detector Data*, University of Göttingen, Germany, 1997.

39 O. V. Dolomanov, L. J. Bourhis, R. J. Gildea, J. A. K. Howard and H. Puschmann, *J. Appl. Crystallogr.*, 2009, **42**, 339–341.

40 M. J. Frisch, G. W. Trucks, H. B. Schlegel, G. E. Scuseria, M. A. Robb, J. R. Cheeseman, G. Scalmani, V. Barone, B. Mennucci, G. A. Petersson, H. Nakatsuji, M. Caricato, X. Li, H. P. Hratchian, A. F. Izmaylov, J. Bloino, G. Zheng, J. L. Sonnenberg, M. Hada, M. Ehara, K. Toyota, R. Fukuda, J. Hasegawa, M. Ishida, T. Nakajima, Y. Honda, O. Kitao, H. Nakai, T. Vreven, J. A. Montgomery Jr, J. E. Peralta, F. Ogliaro, M. Bearpark, J. J. Heyd, E. Brothers, K. N. Kudin, V. N. Staroverov, R. Kobayashi, J. Normand, K. Raghavachari, A. Rendell, J. C. Burant, S. S. Iyengar, J. Tomasi, M. Cossi, N. Rega, J. M. Millam, M. Klene, J. E. Knox, J. B. Cross, V. Bakken, C. Adamo, J. Jaramillo, R. Gomperts, R. E. Stratmann, O. Yazyev, A. J. Austin, R. Cammi, C. Pomelli, J. W. Ochterski, R. L. Martin, K. Morokuma, V. G. Zakrzewski, G. A. Voth, P. Salvador, J. J. Dannenberg, S. Dapprich, A. D. Daniels, Ö. Farkas, J. B. Foresman, J. V. Ortiz, J. Cioslowski and D. J. Fox, *Gaussian 09, Revision D.01*, Gaussian, Inc., 2009.

41 J. B. Paine and D. Dolphin, *J. Org. Chem.*, 1988, **53**, 2787–2795.

42 G. Anguera, B. Kauffmann, J. I. Borrell, S. Borros and D. Sanchez-Garcia, *J. Org. Chem.*, 2017, **82**, 6904–6912.

43 J. Zhou, W. Zhang, X.-F. Jiang, C. Wang, X. Zhou, B. Xu, L. Liu, Z. Xie and Y. Ma, *J. Phys. Chem. Lett.*, 2018, **9**, 596–600.

44 C.-M. Che, C.-W. Wan, W.-Z. Lin, W.-Y. Yu, Z.-Y. Zhou, W. Y. Lai and S. T. Lee, *Chem. Commun.*, 2001, 721–722.

45 D. Birnbaum and B. E. Kohler, *J. Chem. Phys.*, 1991, **95**, 4783–4789.

46 *CRC Handbook of Chemistry and Physics*, ed. D. R. Lide, CRC Press, Boca Raton, FL, 85th edn, 2004.